POLISH POLAR RESEARCH
vol. 24, no. 3–4, pp. 217–242, 2003

Origin of "cannon-ball" concretions in the Carolinefjellet Formation (Lower Cretaceous), Spitsbergen

Krzysztof P. KRAJEWSKI and Bartłomiej LUKS

Instytut Nauk Geologicznych PAN, ul. Twarda 51/55, 00-818 Warszawa, Poland
<kpkraj@twarda.pan.pl>, <luks@acn.waw.pl>

ABSTRACT: Ball-shaped concretions ("cannon balls") commonly occur in a marine, organic carbon-rich sedimentary sequence (Innkjegla Member) of the Carolinefjellet Formation (Aptian–Albian) in Spitsbergen. The sedimentologic, petrographic and geochemical investigation of these concretions in the Kapp Morton section at Van Mijenfjorden gives insight into their origin and diagenetic evolution. The concretion bodies commenced to form in subsurface environment in the upper part of the sulphate reduction (SR) diagenetic zone. They resulted from pervasive cementation of uncompacted sediment enriched in framboidal pyrite by non-ferroan (up to 2 mol% $FeCO_3$) calcite microspar at local sites of enhanced decomposition of organic matter. Bacterial oxidation of organic matter provided most of carbon dioxide necessary for concretionary calcite precipitation ($\delta^{13}C_{CaCO3} \approx -21‰$ VPDB). Perfect ball-like shapes of the concretions originated at this stage, reflecting isotropic permeability of uncompacted sediment. The concretion bodies cracked under continuous burial as a result of amplification of stress around concretions in a more plastic sediment. The crack systems were filled by non-ferroan (up to 5 mol% $FeCO_3$) calcite spar and blocky pyrite in deeper parts of the SR-zone. This cementation was associated with impregnation of parts of the concretion bodies with microgranular pyrite. Bacterial oxidation of organic matter was still the major source of carbon dioxide for crack-filling calcite precipitation ($\delta^{13}C_{CaCO3} \approx -19‰$ VPDB). At this stage, the "cannon-ball" concretions attained their final shape and texture. Subsequent stages of concretion evolution involved burial cementation of rudimentary pore space with carbonate minerals (dolomite/ankerite, siderite, calcite) under increased temperature ($\delta^{18}O_{Ca,Mg,FeCO3} \approx -14‰$ VPDB). Carbon dioxide for mineral precipitation was derived from thermal degradation of organic matter and from dissolution of skeletal carbonates ($\delta^{13}C_{Ca,Mg,FeCO3} \approx -8‰$ VPDB). Kaolinite cement precipitated as the last diagenetic mineral, most probably during post-Early Cretaceous uplift of the sequence.

Key words: Arctic, Svalbard, Lower Cretaceous, "cannon-ball" concretions, diagenesis.

Introduction

"Cannon balls" is an informal name used by Svalbard geologists to describe spherical concretions that occur in organic carbon (OC)-rich, fine-grained intervals of the Mesozoic sedimentary sequence in the archipelago. These concretions,

Fig. 1. Sketch map of Svalbard Archipelago showing location of Kapp Morton at the northern margin of Van Mijenfjorden in Spitsbergen.

usually 5–30 cm in diameter, can be observed in many coastal cliff exposures of the OC-rich rocks, where they remind old cannon balls lodged in city walls. "Cannon-ball" concretions are particularly well-developed in OC-rich, shaly interval of the Lower Cretaceous Carolinefjellet Formation in Spitsbergen, which is classified as the Innkjegla Member (Harland 1997, Mørk *et al*. 1999). Striking appearance, perfect shapes, and easiness of separation from the host rock provide that

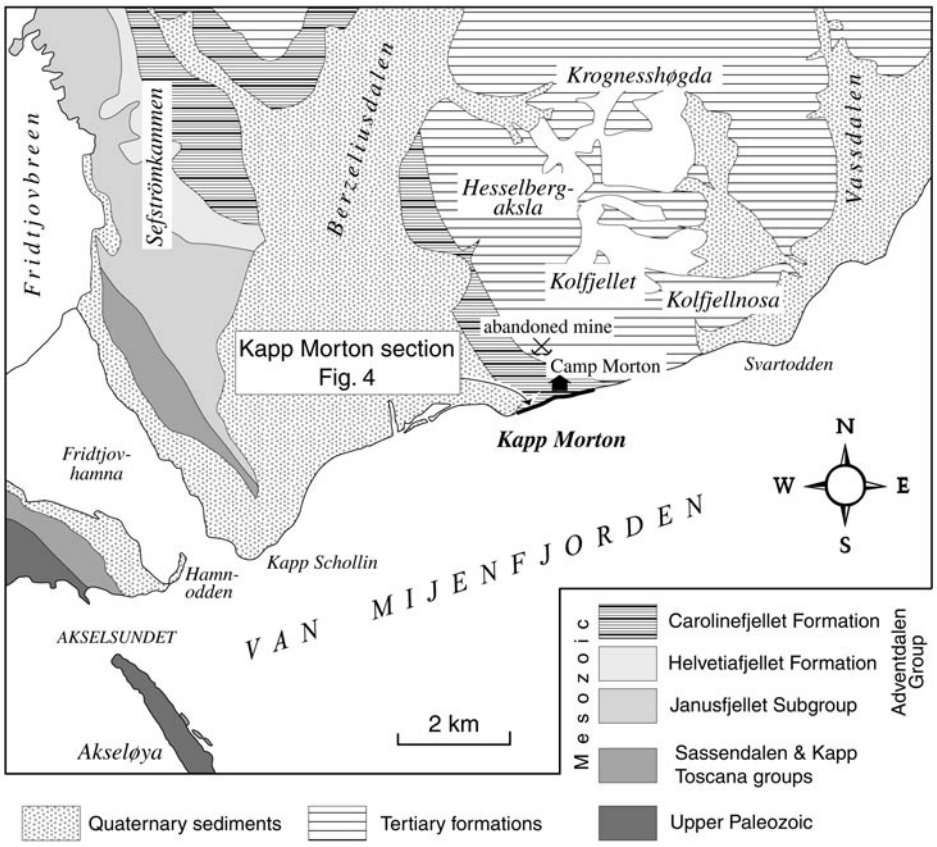

Fig. 2. Geological map of a part of the northern margin of Van Mijenfjorden and location of Kapp Morton section of the Carolinefjellet Formation. Geology after Hjelle *et al*. (1986), simplified.

they became parts of many geological collections and museum exhibitions from the Arctic. However, the nature of their formation has not been a subject of scientific publication.

This paper involves sedimentologic, petrographic and geochemical methods to explain origin and diagenetic history of "cannon-ball" concretions in the Carolinefjellet Formation. It is based on material collected along section of the formation exposed in coastal cliffs at Kapp Morton in Van Mijenfjorden (Fig. 1).

Geological setting

The Carolinefjellet Formation (Aptian–Albian) is the uppermost formation classified into the Jurassic–Cretaceous Adventdalen Group in Svalbard (Mørk *et al*. 1999). It terminates the Mesozoic sedimentary sequence in the archipelago, being overlain by Tertiary sequence of the Van Mijenfjorden Group. The formation em-

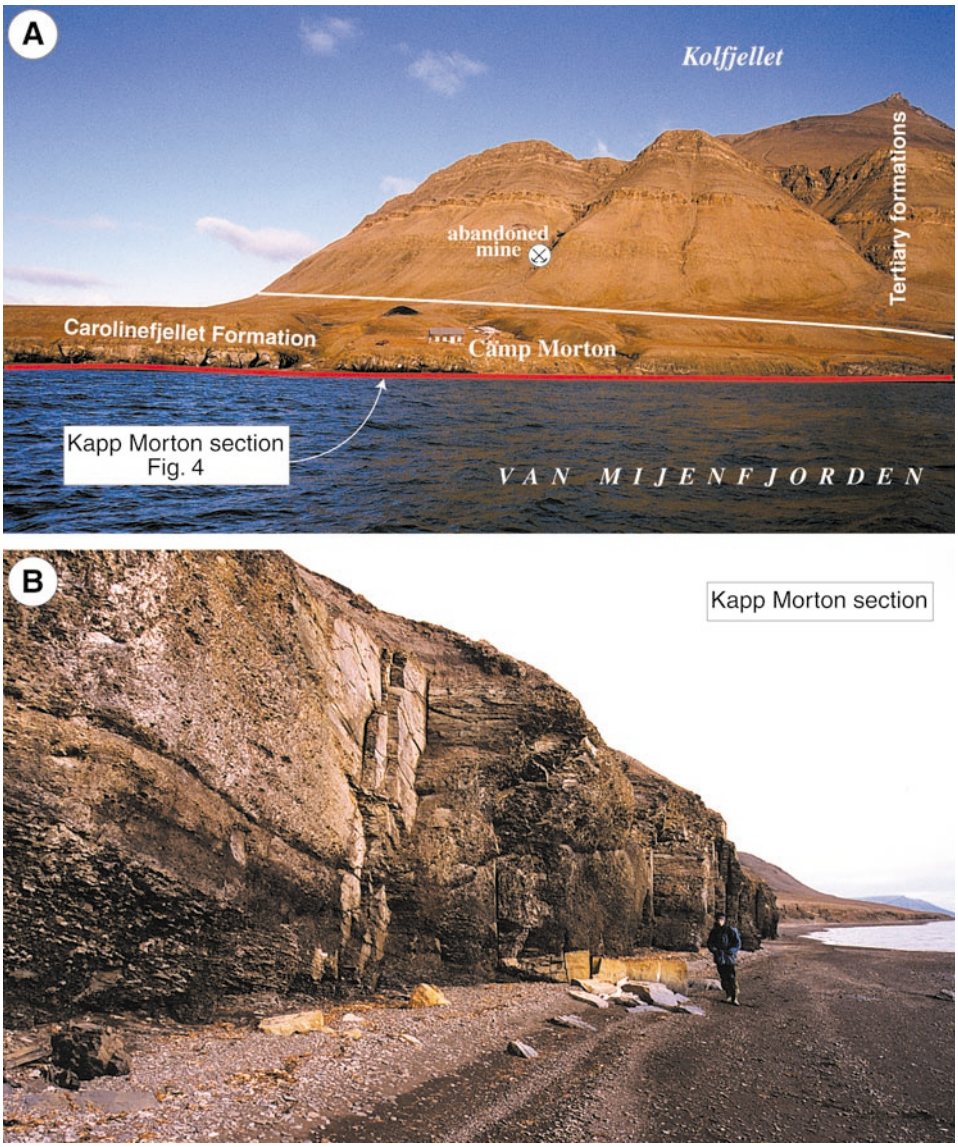

Fig. 3. **A**. Section of the Carolinefjellet Formation in coastal cliffs at Kapp Morton. The Carolinefjellet Formation (Innkjegla Member) terminates the Jurassic–Cretaceous Adventdalen Group sequence in Van Mijenfjorden, and is disconformably overlain by coal-bearing Tertiary formations of the Van Mijenfjorden Group. **B**. Coastal cliffs at Kapp Morton showing gently dipping eastwards strata of the Carolinefjellet Formation (Innkjegla Member). The sequence of dark grey to black muddy to silty shale with common concretionary horizons contains yellow-weathering lense-like cementstone bodies.

braces three units of member rank that occur in stratigraphic order, *i.e.* the Dalkjegla, the Innkjegla, and the Langstakken members, as well as two local units (Zillerberget and Schönrockfjellet members) that constitute the uppermost part of the formation

in SE Spitsbergen (Parker 1967, Nagy 1970). Basal disconformity of the Tertiary sequence cuts discordantly various levels of the Carolinefjellet Formation owing to unequal uplift and erosion during Late Cretaceous (Harland 1997).

The shale-dominated Innkjegla Member is the youngest unit of the Carolinefjellet Formation preserved in the southern part of Nordenskiöld Land in Spitsbergen (Fig. 1). It crops out along a NNW-SSE stretching belt east of Fridtjovbreen (Fig. 2) that forms a part of Tertiary monoclinal structure gently dipping eastwards (Hjelle *et al*. 1986). The best outcrops are those in coastal cliffs at Kapp Morton in Van Mijenfjorden (Fig. 3).

The section at Kapp Morton shows an approximately 250 m thick sequence of OC-rich, dark to black shales, mudstones and siltstones with subordinate sandstone intercalations, representing prodelta and shelf sedimentary facies (Fig. 4). There are recurrent intervals in the sequence enriched in or dominated by diagenetic mineral deposits, out of which four distinct morphogenetic types can be discerned: (*i*) "cannon-ball" concretions, 5–20 cm in diameter; (*ii*) ellipsoidal to parallel-elongated concretions showing massive, zoned, and/or septarian internal structure, 20 cm – 1.5 m along horizontal axis; (*iii*) lense-like cementstone bodies displaying relict primary lamination, usually cross-bedding of sandy sediment, up to 2.5 m thick and 8 m long; and (*iv*) horizontal cementstone bands, either massive or displaying relict primary lamination, up to 1 m thick. These deposits consist of varying mixture of carbonate minerals, including calcite, dolomite/ankerite and siderite, representing displacive cementations of the host sediment. They originated during and after depositional history of the Carolinefjellet Formation, starting from subsurface syngenetic environment down to deep-burial one associated with Paleogene subsidence and tectonic and thermal events in Svalbard.

Occurrence of "cannon-ball" concretions

"Cannon-ball" concretions tend to concentrate at seven intervals along the Kapp Morton section that show thickness from 2 to 4 m (MO-3, 4, 5, 8, 12, 16, and 21 sampling locations; see Fig. 4). The content of concretions in these intervals varies considerably, from rare, randomly distributed concretions to densely packed horizons (Fig. 5). The intervals embrace various types of host sediment, including paper-shale, muddy to silty shale, silty mudstone, siltstone, and sandy siltstone. Despite petrographic variation, the host sediment invariably shows warping of lamination around the concretions, suggesting their early, syngenetic formation throughout the section studied. All the observed concretions represent a pristine variety, i.e. they occur at their original growth position within the sediment, without traces of subsequent reworking or other dynamic concentration processes. This suggests that their distribution in the sequence reflects changing intensity of processes that led to punctuated precipitation of mineral phase during sedimentation of the Carolinefjellet Formation. Enhanced formation of the concretions

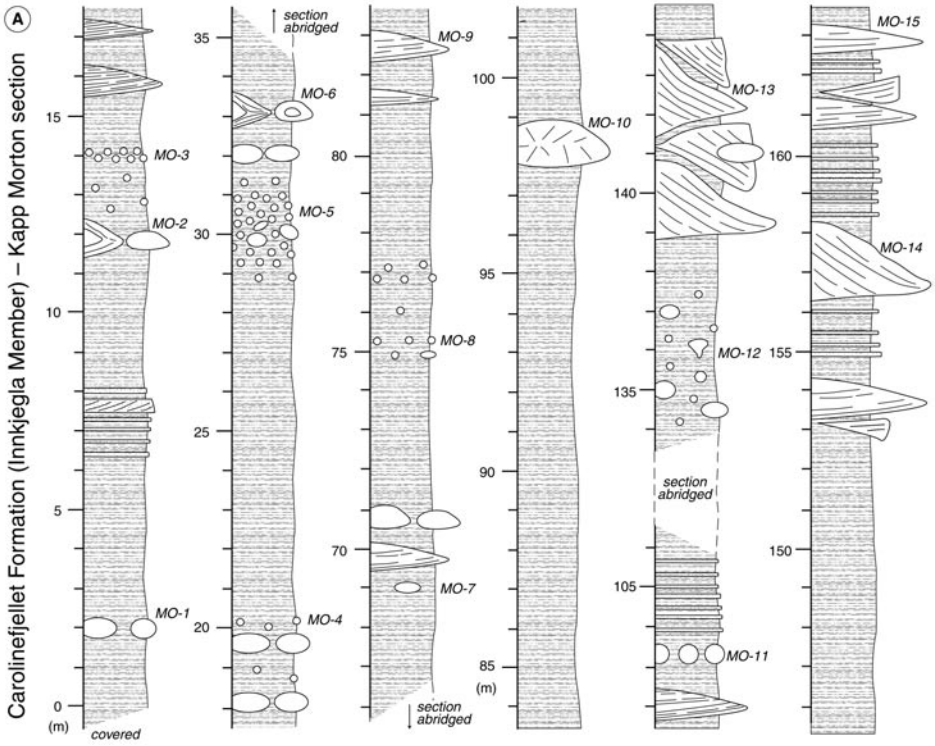

Fig. 4**A**, **B**. Section of the Carolinefjellet Formation (Innkjegla Member) in coastal cliffs at Kapp Morton in Van Mijenfjorden. 1 – muddy to silty shale, paper-shale, subordinate siltstone with sandy layers; 2 – sandstone; 3 – "cannon-ball" (carbonate) concretions; 4 – massive carbonate concretions (ellipsoidal to parallel-elongated in shape); 5 – zoned carbonate concretions (ellipsoidal to parallel-elongated in shape); 6 – carbonate concretions with conspicuous septarian cracks (ellipsoidal to parallel-elongated in shape); 7 – lense-like carbonate cementstone bodies displaying relict primary lamination (usually cross-bedding of sandy sediment); 8 – cementstone bands, either massive or displaying relict primary lamination; 9 – sampling locations. For other explanations see the text.

in subsurface environment during events of suppressed or halted sedimentation is a likely scenario, though direct evidence of this relationship is lacking.

The vast majority of "cannon-ball" concretions have regular spherical shapes, though some are slightly elongated horizontally or vertically, and some show cylindrical or kidney-like shapes. The concretions show dark-grey, dark-green, black or navy blue colours of carbonate bodies on fresh broken surfaces. Many concretions display more or less regular crack systems in their interior. The crack systems are combinations of septarian and spherical cracks that are filled by one or more mineral precipitates. Conspicuous are yellow-sparkling pyrite infillings, though carbonate and clay mineral ones are also common. This evidences that, despite early formation of concretion bodies, the "cannon balls" record far longer diagenetic history related to burial of the Carolinefjellet Formation.

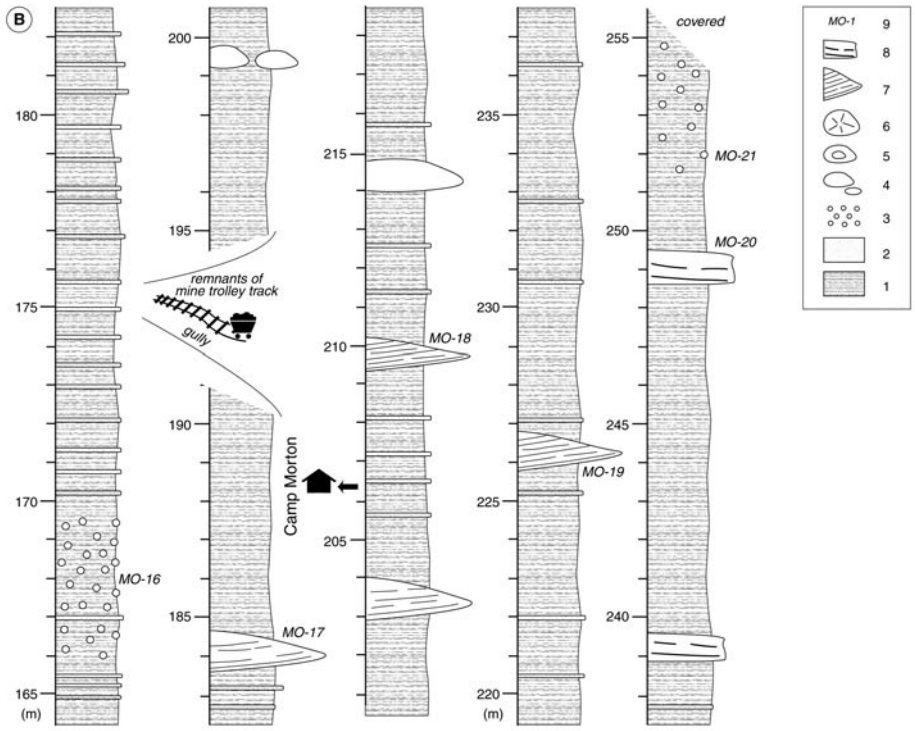

Materials and methods

Eighteen "cannon-ball" concretions from sampling locations MO-3, 4, 5, 8, 12, 16, and 21 (Fig. 4) were cut with a diamond saw, and their sections were analysed using binocular microscope. Selected concretions were analyzed using standard petrographic methods, including transmitted (TLM) and reflected light microscopy (RLM), scanning electron microscopy (SEM), back-scattered electron imaging (BSE), and energy-dispersive X-ray spectroscopy (EDS). Some samples of the concretions were treated with a mixture of 1N acetic acid and ethanol (90:10 wt.%) in order to remove calcitic cement.

Mineral composition of the concretions and the host rock was analyzed by means of X-ray diffraction. Samples were ground to < 63 μm fraction using an agate mortar and pestle. Diffraction patterns were recorded on a SIGMA 2070 diffractometer using a curved position sensitive detector in the range 2–120° 2θ with CoKα radiation and 20 hour analysis time. DIFFRACTIONEL software v. 03/93 was used to process the obtained data.

Quantitative EDS analyses of calcite and pyrite in concretions were obtained using a JEOL JSM-840A scanning electron microscope equipped with a THERMO NORAN VANTAGE EDS system. Operating conditions were a 15 kV acceleration

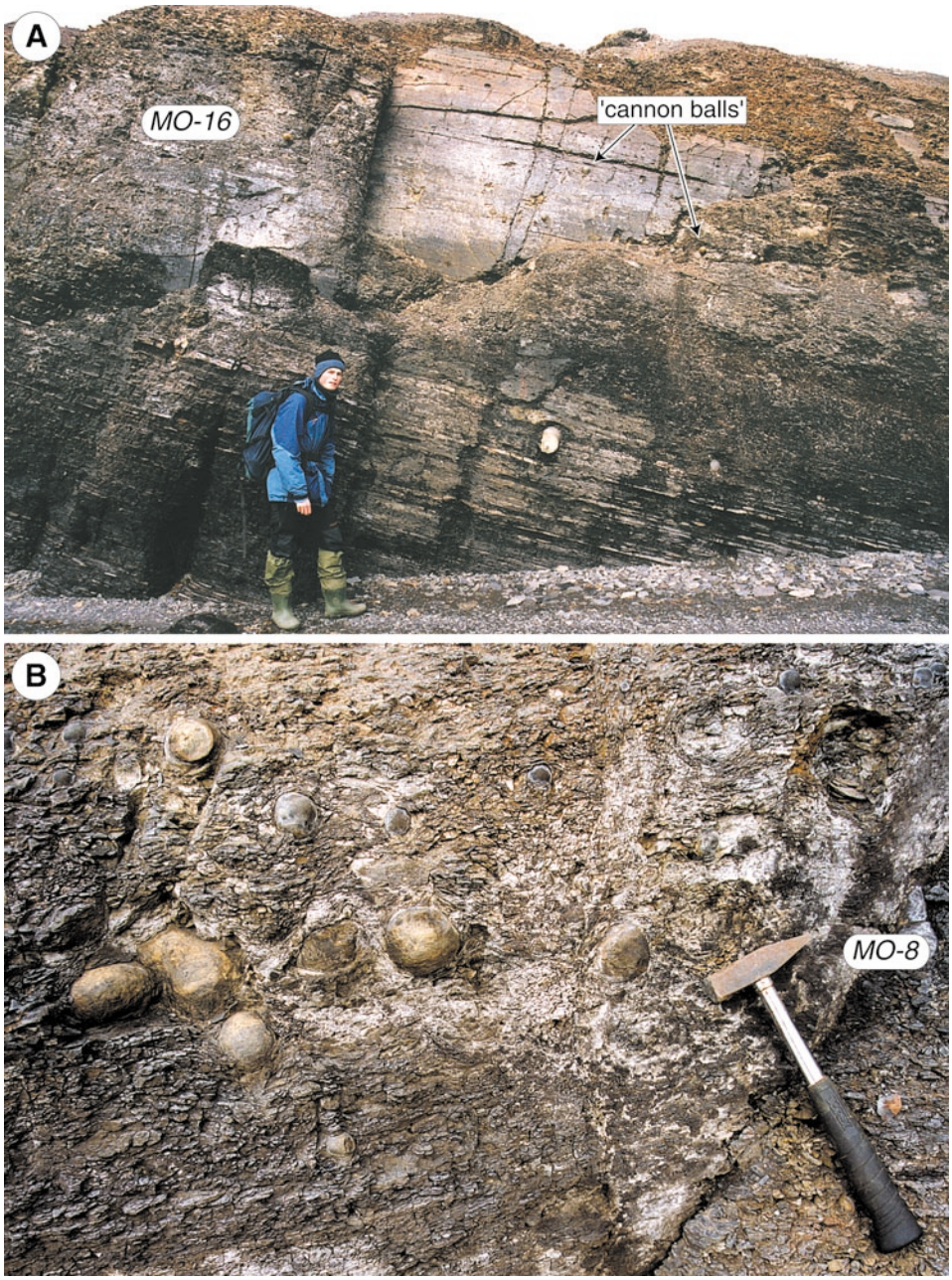

Fig. 5. **A**. Interval containing "cannon-ball" concretions (*MO-16*) in a sequence of dark, muddy siltstone with thin sandstone intercalations. The strata dip gently eastwards. **B**. Horizon of "cannon-ball" concretions (*MO-8*) in black paper-shale. Note the shale layering warping around concretions. Hammer is 40 cm long. A, B – for location in the Kapp Morton section see Fig. 4.

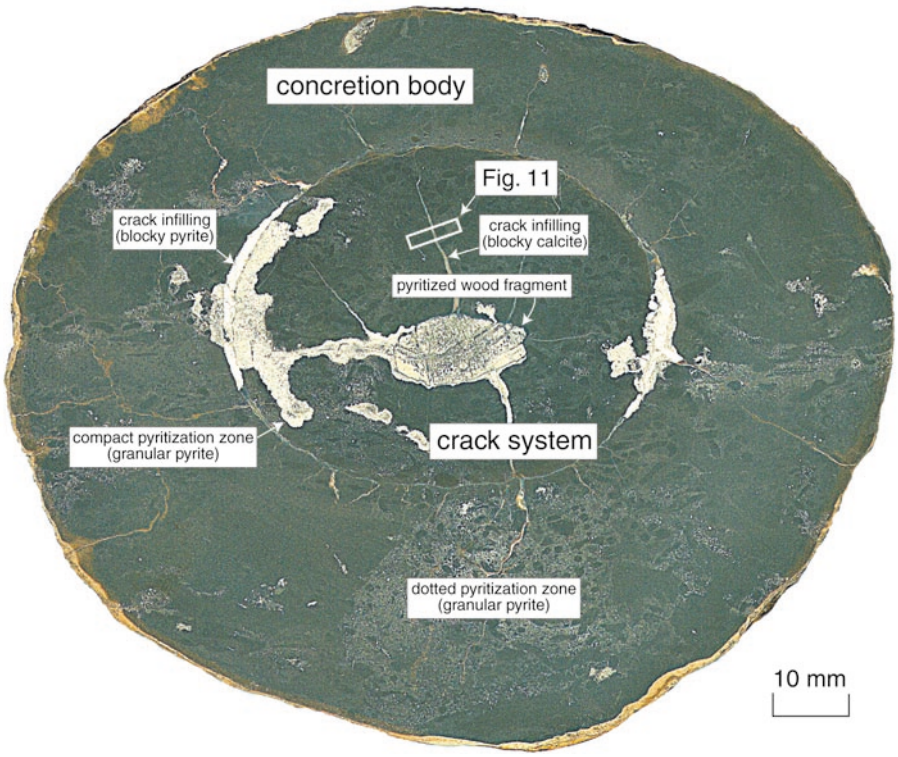

Fig. 6. Vertical axial section of "cannon-ball" concretion from MO-5 sampling location. Polished surface photograph. For location in the Kapp Morton section see Fig 4; for other explanations see the text.

voltage, 1 to 5 μm beam diameter, and 100 s counting time. Detection limits of the analyzed elements (Ca, Mg, Fe, Mn, Co, Ni, Cu, Cd, and S) were better than 0.05 wt%. To facilitate comparison among samples, the EDS data for calcite and pyrite were recalculated as cation mole fractions and weight percent contents, respectively.

Three concretions from sampling locations MO-3, MO-5, and MO-8 were analyzed for the carbon and oxygen isotopic composition of carbonate minerals. The concretion body and crack infilling were analyzed separately. Crushed concretion fragments were hand picked under a binocular microscope to provide material with maximum content of carbonate minerals. CO_2 for isotopic analyses was produced from samples by reaction with anhydrous phosphoric acid (d = 1.90 g cm^{-3}) under vacuum. In an attempt to discriminate between end members of carbonate mixtures, the samples were treated using a progressive acid extraction, with a time sequence of CO_2 collecting. CO_2 from samples containing calcite was collected after 20 hours of reaction at 25° C. CO_2 from samples containing calcite and dolomite/ankerite was collected after 4 h of reaction at 25° C, and after 24 h at 50° C, with a portion of gas discarded after 20 h at 25° C. CO_2 from samples containing

calcite, dolomite/ankerite, and siderite was collected after 4 h of reaction at 25° C, after 24 h at 25° C, and after 72 h at 50° C, with portions of gas discarded after 20 h at 25° C and after 48 h at 50° C. CO_2 collected in these steps represents mostly calcite, dolomite/ankerite, and siderite, respectively. Oxygen isotope fractionation factors $\alpha = 1.01025$ (25° C), $\alpha = 1.01098$ (25° C), 1.01057 (50° C), and $\alpha = 1.01079$ (50° C) were used for calcite, dolomite/ankerite, and siderite, respectively (Becker and Clayton 1976, Rosenbaum and Sheppard 1986, Carothers *et al*. 1988). The same procedure was applied to one sample of host rock collected close to the analysed concretion from sampling location MO-3.

Isotopic $^{13}C/^{12}C$ and $^{18}O/^{16}O$ ratios were determined using a FINNIGAN MAT DELTA^{PLUS} spectrometer working in dual inlet mode with universal triple collector. The δ values were calculated relative to isotopic ratios of the international standard NBS 19. The results are expressed as $\delta^{13}C$ and $\delta^{18}O$ notations with respect to VPDB (Vienna Peedee Belemnite). Analytical reproducibility in laboratory was better than ± 0.05‰ and ± 0.1‰ for $\delta^{13}C$ and $\delta^{18}O$, respectively.

Results

Petrography. — All the examined sections of "cannon-ball" concretions show uncompacted texture of relict sediment throughout the concretion bodies (Fig. 6). Bioturbations and faecal pellets are commonly observed. The exception is the very margins of concretions contacting the host rock, where these sedimentary features are flattened and mechanically deformed.

The concretion bodies consist of a massive matrix composed of clastic components, organic detritus, dispersed pyrite, and carbonate cement. Macroscopic wood fragments or uncrushed fossils are found to occupy centres of some axial sections. The proportion of cement varies insignificantly along the sections, without a clear decreasing-outward trend observed in many concentrically zoned concretions. Clastic components within the concretions resemble very closely the ones occurring in the host rock, though they do not show mechanical orientation related to burial compaction (Fig. 7). They range in size from the clay to the sand fraction, with clear predominance of silt-sized material. They are represented by quartz and albite grains, detrital micas, and clay minerals (illite, chlorite) (Fig. 8). Organic matter is dominated by debris of land plants, with amorphous fraction being a noticeable component (Fig. 9A). Pyrite grains are common in the concretion matrix. BSE images document that the grains consist of two pyrite generations: (*i*) framboids occurring in centres of the grains; and (*ii*) granular overgrowths forming their external parts (Fig. 7C). In larger original pores, the concentration of pyrite grains increases, and at places pyrite prevails volumetrically over the calcite cement (Fig. 9B). Similar pyrite grains occur in all host sediment in all investigated concretion-bearing intervals. Pyritized wood fragments present in the con-

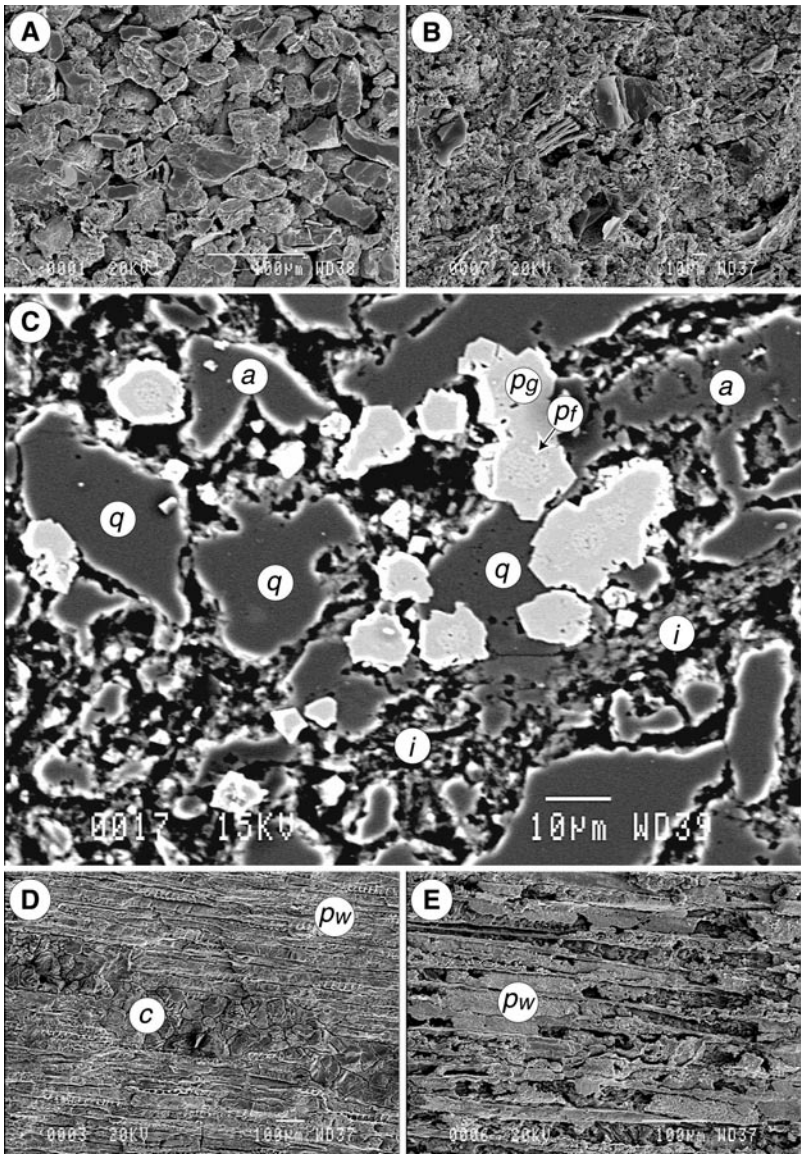

Fig. 7. **A**. Silty sand forming internal sediment in "cannon-ball" concretion at MO-16 sampling location. Detrital grains are dominated by quartz and albite. **B**. Clay dominated internal sediment in "cannon-ball" concretion at MO-8 sampling location. Note the uncompacted nature of the sediment. **C**. Matrix in "cannon-ball" concretion consists of detrital quartz (*q*) and albite (*a*) grains, clay minerals, mostly illite (*i*), and pyrite grains composed of framboids (p_f) and microgranular overgrowths (p_g). These components are cemented by calcitic microspar, which was here artificially dissolved. **D**. Pyritized wood fragment (p_w) in the centre of "cannon-ball" concretion at MO-3 sampling location cut by a crack filled with blocky calcite spar (*c*). **E**. Pyritized wood (p_w) showing preserved cellular structure; MO-3 sampling location. A, B, D, E – SEM photomicrographs of broken concretion surfaces subjected to acid treatment (calcite cement partly dissolved); C – BSE image of acid treated polished section (calcite cement dissolved). For location in the Kapp Morton section see Fig 4.

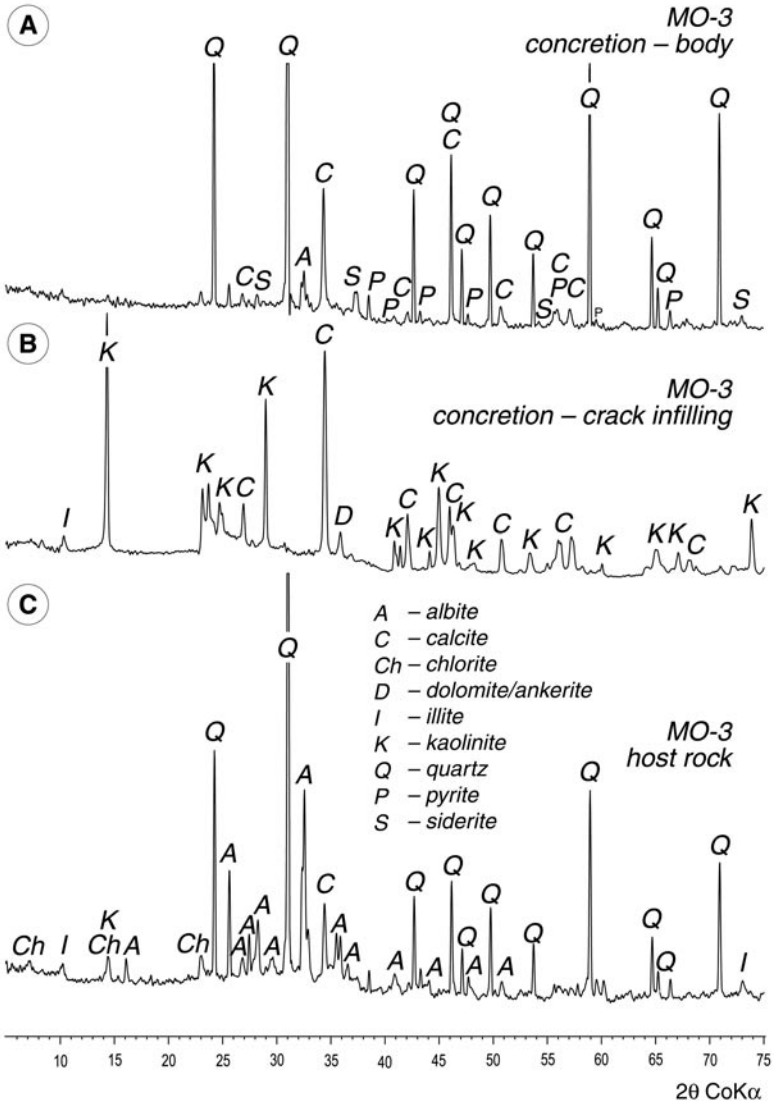

Fig. 8. X-ray diffraction patterns of concretion body (**A**), crack infilling (**B**), and the host sediment (**C**) from sampling location MO-3 in the Kapp Morton section.

cretions show well-preserved cellular structure without any trace of mechanical deformation (Fig. 7D, E).

Clastic components, organic matter, and pyrite grains are cemented by microsparitic to micritic calcite containing, in some concretions, an accessory admixture of dolomite/ankerite and siderite (Fig. 8). Under high magnifications, the matrix usually shows interlocking mosaic of anhedral calcite crystals replacing inter-particle pore space between clastic components and organic debris (Fig. 9A). The

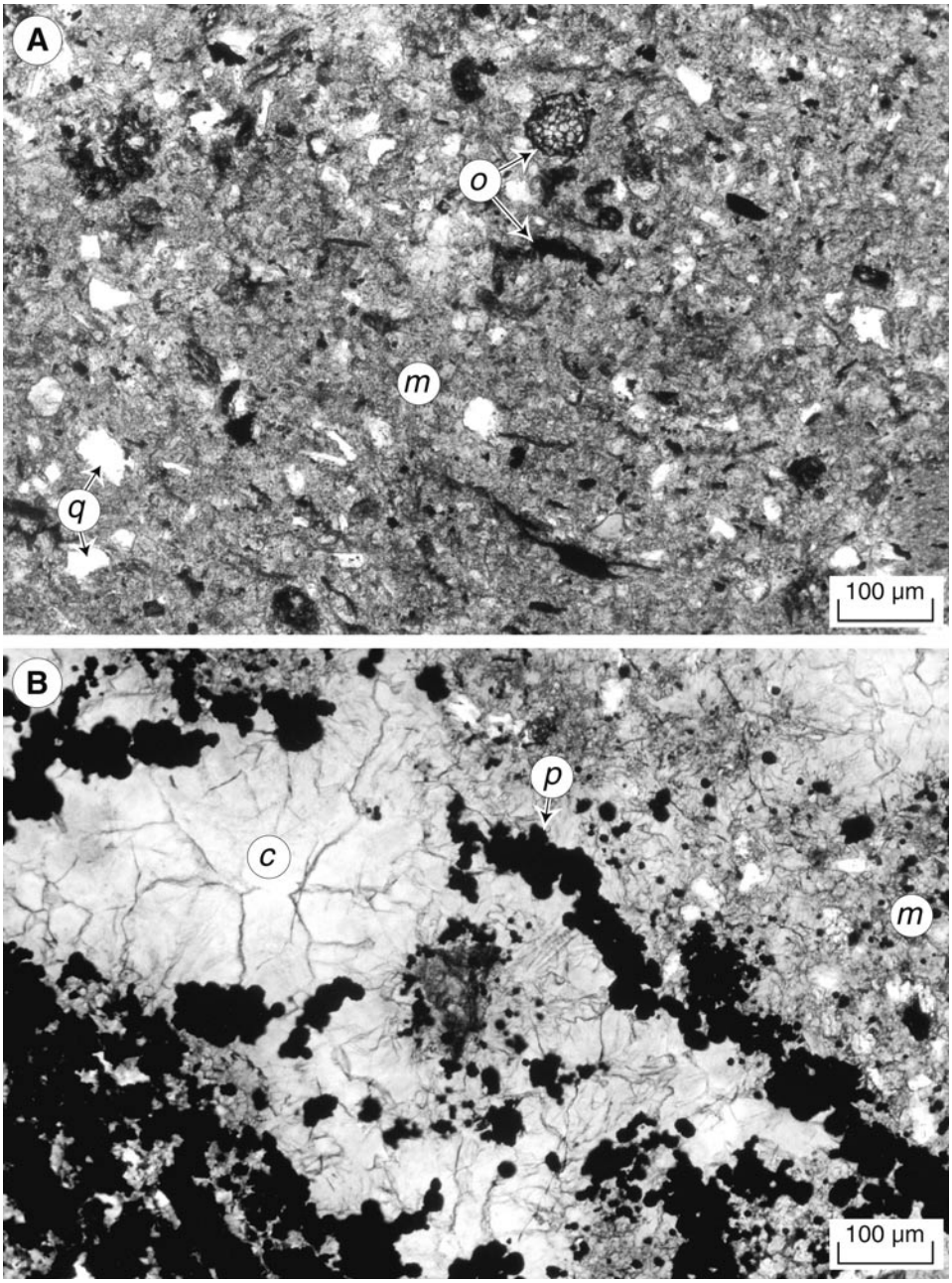

Fig. 9. **A**. Matrix (*m*) in concretion body consists of detrital sediment grains dominated by quartz (*q*), structured and amorphous organic matter (*o*), and clay minerals that are cemented by calcite microspar. **B**. Larger original pores in the concretion matrix (*m*) tend to concentrate composite pyritic grains (*p*), and are cemented with calcite spar (*c*) A, B – TLM photomicrographs of thin sections, normal light. MO-5; for location in the Kapp Morton section see Fig 4.

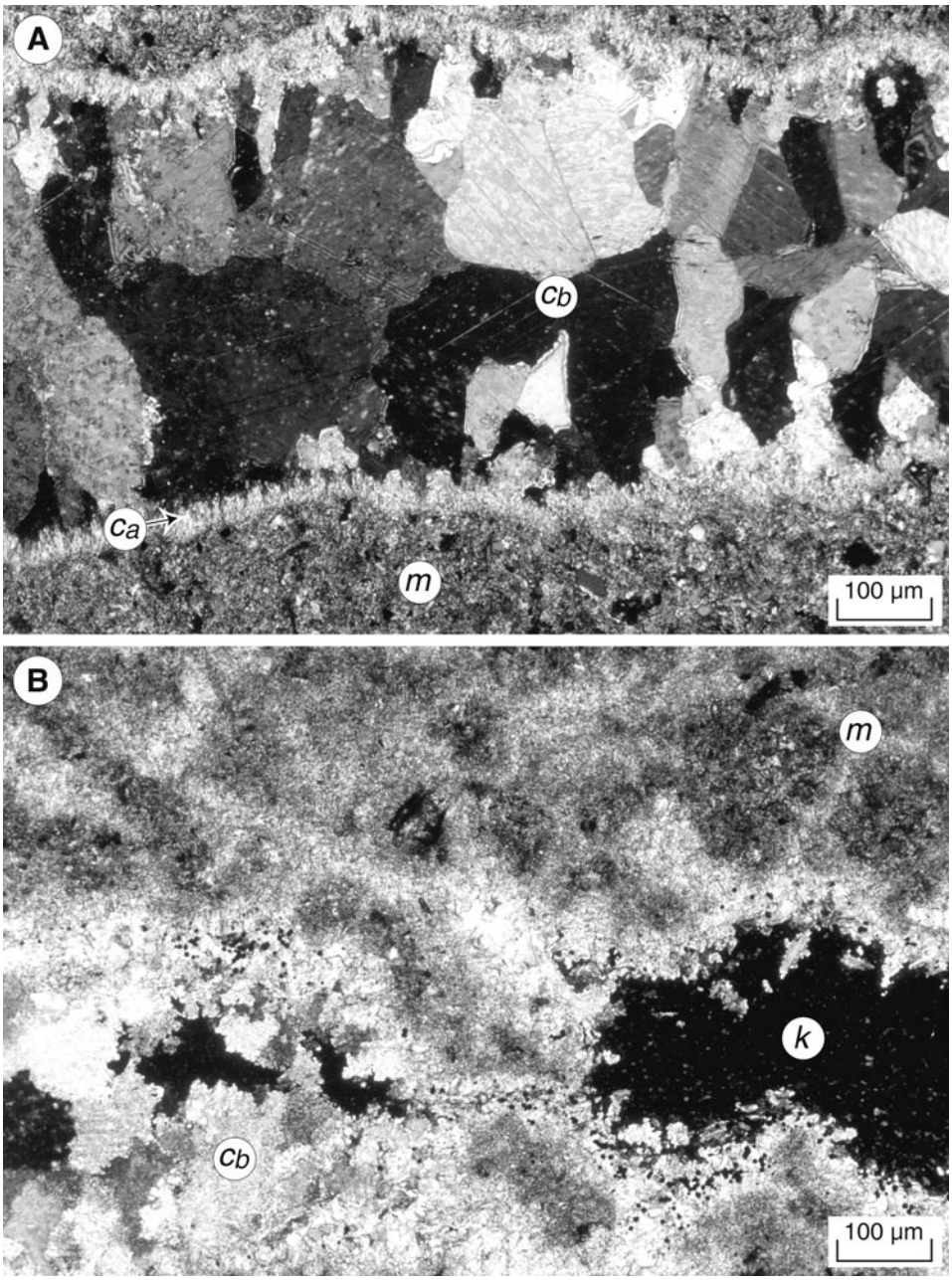

Fig. 10. **A**. Calcite-filled crack has sharp edges towards the concretion matrix (*m*), and shows paragenetic sequence of acicular calcite (c_a) and blocky calcite (c_b). **B**. Crack in a concretion filled with blocky calcite (c_b) and vermicular kaolinite (*k*). Note the pelloidal nature of the concretion matrix (*m*). A, B – TLM photomicrographs of thin sections, nicols crossed. MO-3; for location in the Kapp Morton section see Fig 4.

Table 1

Chemical composition of calcite in "cannon-ball" concretion in the Kapp Morton section of the Carolinefjellet Formation. MO-5 sampling location.

Analysis		$CaCO_3$	$MgCO_3$	$FeCO_3$	$MnCO_3$
		(mol%)			
1	Concretion body (microspar)	97.17	1.46	1.32	0.05
2		96.82	1.16	1.60	0.42
3		96.91	1.11	1.52	0.45
4		96.41	0.84	2.03	0.72
5		97.54	1.35	0.47	0.64
6		95.70	1.53	2.26	0.52
7		98.26	1.51	0.11	0.12
8		96.10	1.08	2.15	0.66
9		96.50	0.83	2.17	0.50
10		95.76	1.05	2.39	0.80
11	Crack infilling (spar)	92.63	2.41	4.22	0.73
12		92.55	2.63	4.20	0.61
13		91.57	2.39	5.22	0.81
14		92.41	2.22	5.05	0.32
15		92.13	2.02	5.25	0.60
16		92.31	2.42	4.54	0.73
17		92.55	2.63	4.47	0.36
18		91.66	2.50	5.03	0.80
19		95.59	0.95	2.80	0.66
20		93.35	1.54	4.55	0.56

calcitic mosaic also incorporates minute inclusions of organic matter and clay minerals. In larger original pores, the cement is developed as calcite spar, with many crystals showing subhedral shapes (Fig. 9B).

The cracks in "cannon-ball" concretions are filled either by calcite or pyrite, or show they complex intergrowths of the two (Fig. 6). Many calcitic infillings display a paragenetic sequence of (*i*) acicular calcite that fringes the crack surfaces, and (*ii*) blocky calcite (mostly subhedral) that fills up the cracks growing from the margins inwards (Fig. 10A). Some show only the blocky calcite replacing completely or incompletely the crack space (Figs 7D, 10B). X-ray survey documents that the calcite spar contains an admixture of dolomite/ankerite and siderite (Fig. 8), though these mineral phases have not been identified microscopically. Pyrite filling cracks displays blocky to massive microfabric. Cracks that are filled both by calcite and pyrite suggest that the major stage of calcite precipitation pre-dated the major stage of pyrite precipitation. Pyrite-filled cracks are closely associated with pyritization zones that extend outward into the concretion body (Fig. 6). There can be distinguished two types of pyritization zones: (*i*) compact pyritization zones that consist of densely packed granular pyrite crystals; and (*ii*) dotted pyritization

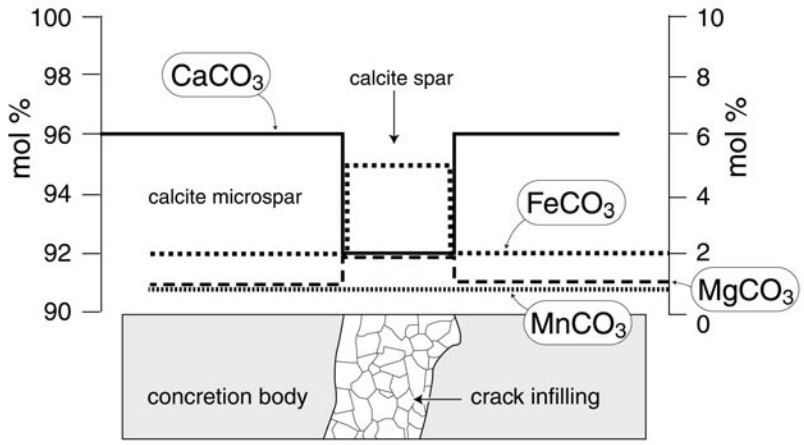

Fig. 11. Compositional difference between calcite microspar cementing matrix in concretion body and calcite spar infilling crack. MO-5; for location in the concretion section see Fig. 6; For source data see Table 1.

zones, in which granular pyrite crystals show mosaic to patchy distribution. Compact pyritization zones tend to concentrate in the concretion centres, whereas the dotted ones form irregular impregnations in their external parts.

Rudimentary pore space in the crack systems that remained open after calcite/pyrite precipitation was subsequently infilled by vermicular aggregates of kaolinite (Figs 8, 10B). Kaolinite terminates the paragenetic mineral sequence revealed in the "cannon-ball" concretions.

Geochemistry. — Calcite forming concretion bodies and crack infillings is a non-ferroan variety of calcite (Table 1). Its mean composition is $(Ca_{0.96}Mg_{0.01}Fe_{0.02}Mn_{0.01})CO_3$ and $(Ca_{0.92}Mg_{0.02}Fe_{0.05}Mn_{0.01})CO_3$, respectively. The paragenetic sequence shows an increase in $FeCO_3$ content (from 2 to 5 mol%) and a negligible increase in $MgCO_3$ content (from 1 to 2 mol%) from the body forming microspar to the crack filling spar (Fig. 11).

Compositional changes among generations of pyrite present in concretions are negligible, though framboidal pyrite shows a slightly elevated content of Ni and Cu (Table 2). Mean content of Ni and Cu in pyritic framboids is 0.3 and 0.4 wt.%, respectively; it drops to less than 0.1 wt.% in microgranular overgrowths of framboids and in blocky pyrite infillings of cracks (Fig. 12).

Carbon and oxygen isotopes. — The obtained $\delta^{13}C$ and $\delta^{18}O$ values for carbonate minerals present in "cannon-ball" concretions as well as for calcite in the host sediment are listed in Table 3.

The $\delta^{13}C$ for calcite microspar forming matrix in concretion bodies varies from –23.4‰ to –19.7‰ VPDB. The $\delta^{18}O$ varies from –6.5‰ to –3.1‰ VPDB. Mean values are –21‰ VPDB and –5‰ VPDB, respectively. The $\delta^{13}C$ for calcite spar infilling cracks in concretions varies from –19.2‰ to –18.5‰ VPDB. The $\delta^{18}O$

Table 2

Chemical composition of pyrite in "cannon-ball" concretion in the Kapp Morton section of the Carolinefjellet Formation. MO-3 sampling location.

Analytical point		S	Fe	Co	Ni	Cu	Cd	Mn
		(weight%)						
A1	Framboidal pyrite	53.32	46.06	–	0.24	0.38	–	–
A2		52.55	46.65	0.05	0.54	0.21	–	–
A3		52.52	46.49	–	0.28	0.55	–	0.16
A4		52.81	46.35	–	0.43	0.41	–	–
A5		53.00	46.30	0.28	–	0.43	–	–
A6	Granular pyrite	53.06	46.80	0.04	0.07	–	–	0.03
A7		52.41	47.59	–	–	–	–	–
A8		52.66	46.87	–	0.22	–	–	0.24
A9		52.77	46.93	–	–	0.31	–	–
A10		52.75	47.19	–	–	–	–	0.06
B1	Blocky pyrite	53.22	46.60	–	–	0.18	–	–
B2		52.78	47.00	–	0.03	0.07	–	0.12
B3		53.12	46.68	–	–	0.15	0.04	–
B4		53.32	46.60	–	–	0.08	–	–
B5		52.65	47.17	0.16	–	–	0.02	–
B6		52.68	47.32	–	–	–	–	–
B7		53.12	46.71	–	0.17	–	–	–
B8		52.72	47.12	–	–	0.16	–	–
B9		53.21	46.66	–	–	–	–	0.13
B10		52.94	47.06	–	–	–	–	–

varies from –6.4‰ to –5.8‰ VPDB. Mean values are –19‰ VPDB and –6‰ VPDB, respectively. These values demonstrate that calcite in the concretions contains isotopically very light carbon, though it evolves towards slightly heavier composition from microsparitic cement to crack-filling spar.

Dolomite/ankerite and siderite, that occur in accessory amounts in crack infillings, show contrasted isotopic composition. The $\delta^{13}C$ varies from –10.8‰ to –5.7‰ VPDB, and the $\delta^{18}O$ from –16.9‰ to –11.8‰ VPDB. Similar values have been obtained for calcite occurring in the form of disseminated cement in the host rock of the MO-3 concretion-bearing interval. The $\delta^{13}C$ and $\delta^{18}O$ are –7.4‰ and –16.6‰ VPDB, respectively.

Discussion

Relict sedimentary structures preserved in "cannon-ball" concretions suggest that the concretion bodies formed by a rather rapid, pervasive calcite cementation

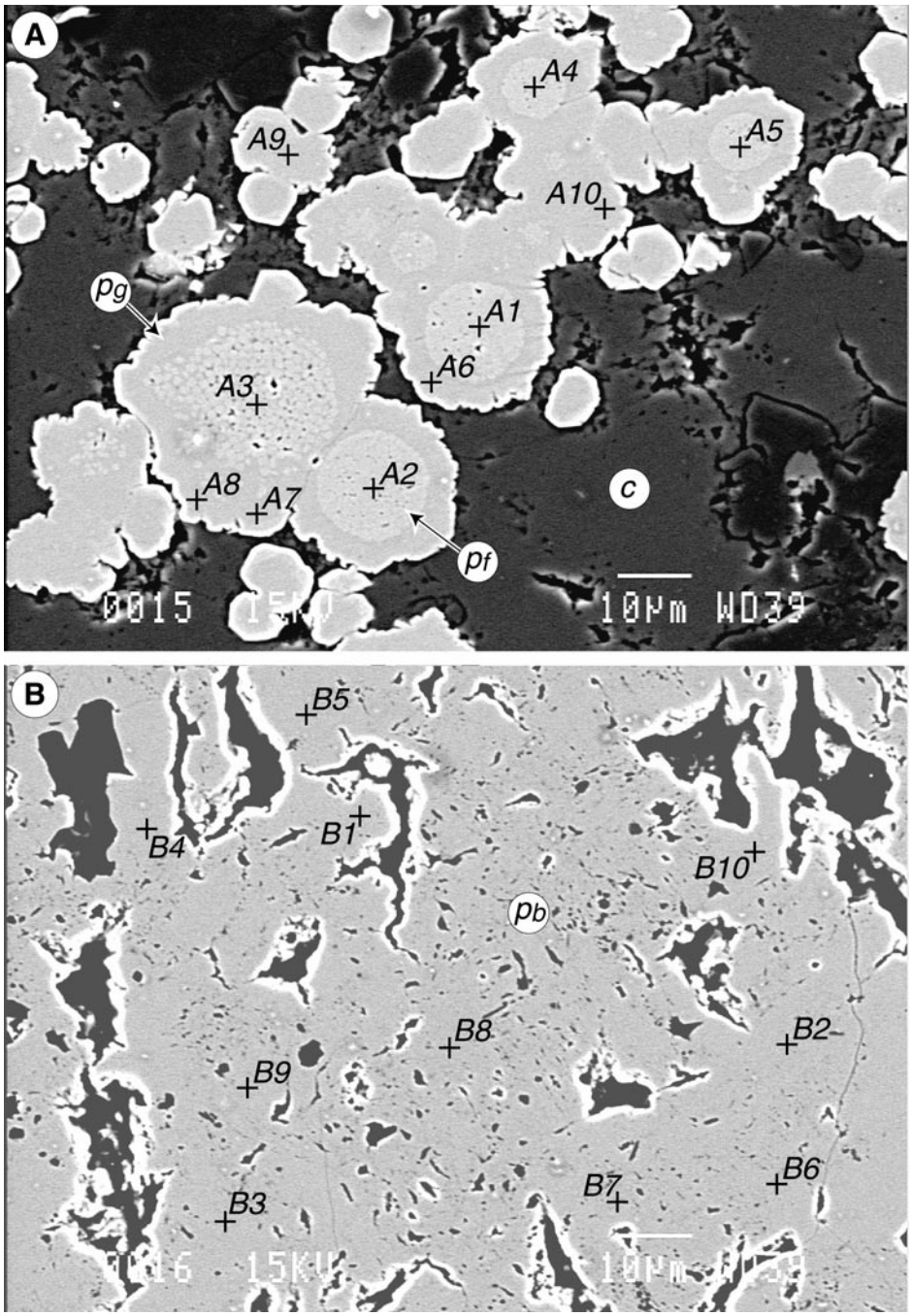

Fig. 12. **A**. Composite pyritic grains consisting of framboids (p_f) and microgranular overgrowths (p_g) in calcite microspar in matrix of a concretion body. **B**. Blocky pyrite (p_b) infilling crack in concretion. A, B – BSE images of polished sections; *A1–A10* and *B1–B10* are analytical microprobe points. MO-3; for location in the Kapp Morton section see Fig 4.

Table 3

Isotopic composition of carbon and oxygen in carbonates forming "cannon-ball" concretions in the Kapp Morton section of the Carolinefjellet Formation.

Analysis	Sample	Mineral phase	Location	$\delta^{13}C$	$\delta^{18}O$
				(‰ VPDB)	
1	MO-3	calcite (microspar)	Concretion body	–20.1	–3.1
2	MO-3	calcite (microspar)		–21.3	–6.4
3	MO-5	calcite (microspar)		–23.4	–4.9
4	MO-5	calcite (microspar)		–23.0	–6.5
5	MO-8	calcite (microspar)		–19.7	–5.3
6	MO-8	calcite (microspar)		–19.8	–5.3
7	MO-3	calcite (spar)	Crack infilling	–18.5	–6.4
8	MO-3	calcite (spar)		–19.2	–6.0
9	MO-5	calcite (spar)		–18.5	–6.4
10	MO-5	calcite (spar)		–18.8	–5.8
11	MO-3	dolomite/ankerite		–8.0	–16.9
12	MO-3	dolomite/ankerite		–10.8	–12.3
13	MO-3	siderite		–5.7	–11.8
14	MO-3	calcite	host rock	–7.4	–16.6

of spherical parts of sediment prior to its noticeable compaction, i.e. at very shallow depths. The actual depth in sediment column at which the "cannon balls" have commenced growth is difficult to estimate, but a few metres, at most, below the water/sediment interface is likely. It seems obvious that the calcite cement grew in the pore space of the sediment and eventually firmly cemented it. Preservation of delicate cellular structure of plant fragments implies that no actual compaction affected the organic debris before the concretion bodies were formed. The dominant ball-like shapes of the concretions imply equal or nearly equal permeability of sediment in vertical and horizontal directions, supporting very shallow formation. Rapid change of structure and fabric at margins of the concretions, which become more clastic and mechanically oriented, suggests that the growth of concretion bodies terminated during incipient stages of compaction.

Pervasive growth of concretions involves simultaneous nucleation and precipitation of a patch of carbonate crystals to form a framework which is resistant to compaction, though it retains much porosity at initial cementation stages (Raiswell and Fisher 2000). Petrographic evidence demonstrates that initial stages of calcite cementation coincided with the formation of framboidal pyrite in the Carolinefjellet sediment. This association is prominent throughout the Kapp Morton section, suggesting the commencement of "cannon ball" formation under high rates of iron sulphide precipitation in the sulphate reduction (SR) diagenetic zone. The development of this zone close to the water/sediment interface is quite typical for OC-rich marine sediments (Berner 1985). In the sediments studied, however,

this zone was overlain by a surficial oxic/suboxic (OX/FeR) diagenetic zone, as it is evidenced by common bioturbations preserved in the concretion bodies. The non-ferroan composition of the microspar (up to 2 mol% $FeCO_3$) is consistent with the formation in the SR-zone, where iron is preferentially sequestered into iron sulphides (Coleman and Raiswell 1993). Continuing calcite cementation in the concretion bodies was associated with a change of dominant type of pyrite, from framboidal to granular. This change suggests a decrease in saturation level with respect to iron sulphides down the SR-zone as a result of decreased availability of dissolved sulphate, reactive iron compounds and/or easily metabolizable organic fractions (Raiswell 1982). Decelerated rates of sulphate reduction were associated with a decrease in metal substitutions in pyrite, which is consistent with slowed mineralization of organic matter down the sediment column.

The material analyzed in this study suggests that crack systems in "cannon balls" developed relatively early during diagenesis of the Carolinefjellet Formation. Among many possible mechanisms of crack formation discussed in the literature (e.g., Astin 1986, Hesselbo and Palmer 1992, Hounslow 1997, Raiswell and Fisher 2000, Pratt 2001), amplification of stress around stiff concretions in a more plastic sediment (Sellés-Martínez 1996) seems to be a likely mechanism for the concretions studied, as it preferentially occurs at shallow burial depths. Calcite spar in the cracks occurs in paragenetic association with massive, blocky and microgranular pyrite, suggesting the crack filling still in the SR-zone, though deeper in the sediment column and at lower intensity of mineral precipitation. This is supported by a higher content of iron in the calcite spar (up to 5 mol% $FeCO_3$) and by pyrite micromorphology. Complex sequences of calcite precipitation, pyrite precipitation, and pyritization of concretion bodies associated with local dissolution of formerly precipitated microspar witness compositional changes and evolution of the concretion microenvironments during early diagenesis.

The calcite carbon is isotopically very light (mean –21‰ and –19‰ VPDB for concretion bodies and crack infillings, respectively), documenting that oxidation of organic matter was the major source of carbon dioxide for mineral precipitation (Fig. 13). The paragenetic sequence of calcite shows an indistinct trend towards slightly heavier carbon from the concretion body to crack infilling, which suggests decreasing influence of sulphate reduction associated with progressive closure of diagenetic environment down the sediment column.

If equilibrium model of calcite formation is assumed, the precipitation temperatures calculated from the obtained $\delta^{18}O$ values for the concretions fall in a range between 10° and 50° C, using the fractionation equation of Friedman and O'Neil (1977) for assumed $\delta^{18}O$ of pore fluids from –5‰ to 0‰ SMOW (Fig. 14). Taking into account a very shallow formation of the "cannon-ball" concretions, it is likely that the pore fluids from which they precipitated had composition close to sea water. Assuming equilibrium precipitation from pore fluids having composition of non-glacial seawater (–1‰ SMOW), the mean $\delta^{18}O$ values for microspar forming

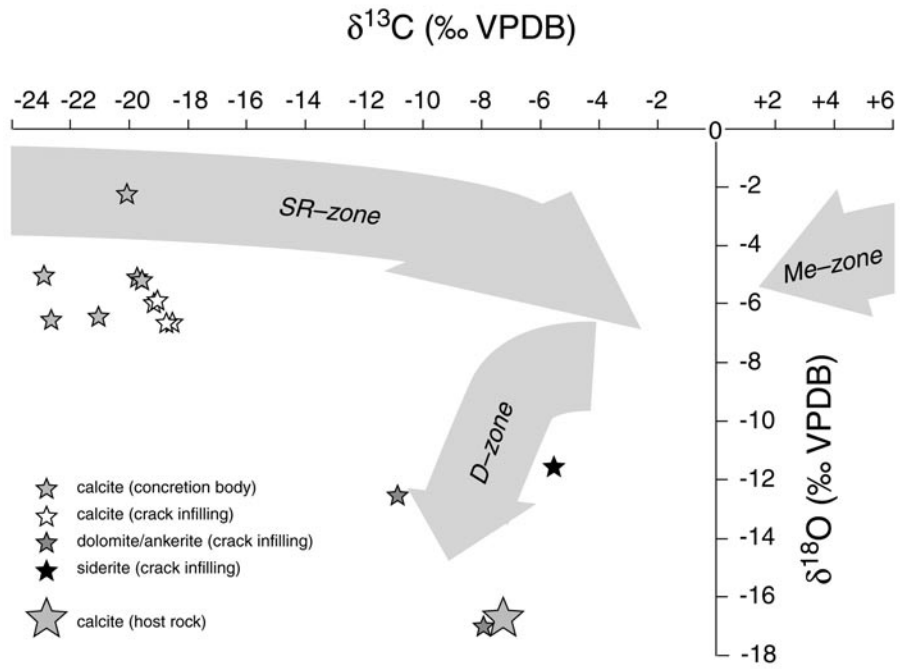

Fig. 13. Plot of $\delta^{13}C$ (‰ VPDB) versus $\delta^{18}O$ (‰ VPDB) of the carbonates in "canon-ball" concretions and the host sediment in the Kapp Morton section. For source data see Table 3. Diagenetic trends in the sulphate reduction zone (*SR-zone*), methanogenic zone (*Me-zone*), and decarboxylation zone (*D-zone*) after Scotchman (1989).

concretion bodies (–5‰ VPDB) and for spar filling cracks (–6‰ VPDB) correspond to a precipitation temperature of 35˚C and 40˚C, respectively. These temperature estimates are clearly too high when we consider sedimentary temperatures in the Carolinefjellet Formation obtained from oxygen isotopic composition of bivalves (6.5–10.1 ˚C; Ditchfield and Staley *in* Harland 1997, p. 381) and a shallow subsurface formation of the concretions. Similar anomaly is observed in many carbonate concretions originated in OC-rich mudrocks, with a number of possible explanations for ^{18}O depletion (Mozley and Burns 1993). The likely scenarios embrace: (*i*) mixing with meteoric water (Scotchman 1991); (*ii*) precipitation at anomalously high temperatures (Astin and Scotchman 1988); and (*iii*) local equilibrium precipitation at isolated sites in the sediment (Coleman and Raiswell 1995). The former two scenarios are unlikely for the studied concretions. The latter one, however, is consistent with common occurrence of organic remains in the concretion centres that clearly defined local geochemical gradients in the sediment during early stages of diagenesis as a result of enhanced degradation of organic matter. Local ^{18}O depletion of carbonate ion might result from the incorporation of ^{18}O-depleted oxygen from sulphate and organic matter during bacterial sulphate reduction (Coleman and Raiswell 1981, Sass *et al*. 1991).

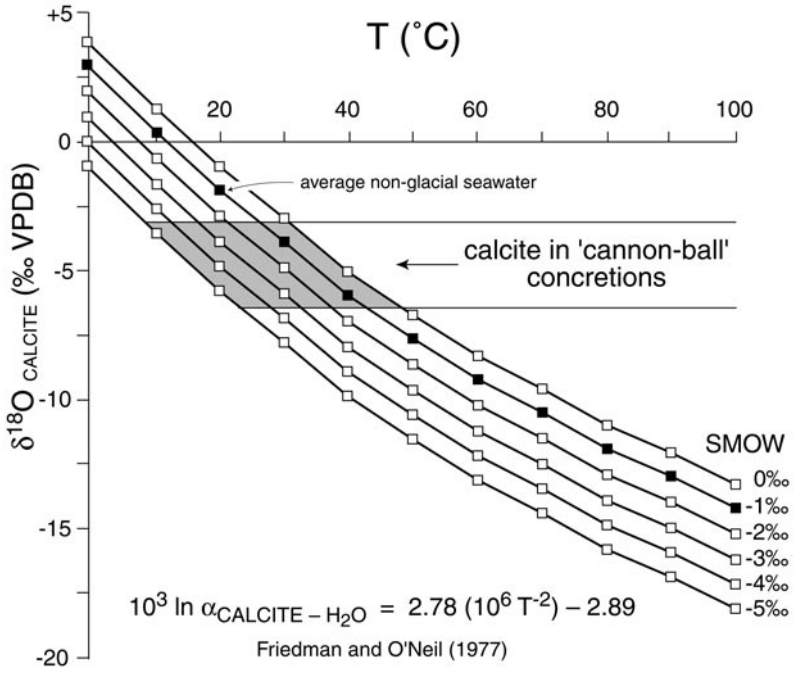

Fig. 14. Range of $\delta^{18}O$ (‰ VPDB) of calcite in "canon-ball" concretions in the Kapp Morton section against precipitation temperature T (°C) of inorganic calcite, with the calculated isotopic composition of diagenetic fluids from which it may have formed, assuming isotopic equilibrium. The water lines were calculated using the fractionation equation of Friedman and O'Neil (1977).

Rudimentary pore space in "cannon-ball" concretions, both in the concretion bodies and in crack systems, was cemented by carbonate minerals during later stages of diagenesis. The carbonates have been X-ray identified to be dolomite/ankerite and siderite, though it is likely that late calcite cement revealed in the host rock also precipitated within the concretions. The $\delta^{13}C$ values for these cements (–11‰ to –7‰ VPDB) indicate a mixed origin of carbonate carbon derived from mineralization of organic matter and from dissolution of skeletal carbonates. They also indicate that mineralization of organic matter occurred either by oxidation or by thermal decomposition processes (Irwin *et al*. 1977). Since these carbonates post-date the concretionary and crack-filling calcite formed in the SR-zone, thermal processes of organic matter decomposition during burial, like decarboxylation, are most likely source of isotopically light carbon (Krajewski *et al.* 2001). This is consistent with strongly negative $\delta^{18}O$ values, typical for carbonates formed in the decarboxylation (D) diagenetic zone and in catagenic environments (Fig. 13). The apparent lack of methanogenic (Me) carbonates noted in "cannon-ball" concretions seems to be a typical feature of diagenetic deposits in OC-rich facies of the Adventdalen Group, suggesting early kerogenization of organic matter throughout the sequence (Krajewski 2002, submitted).

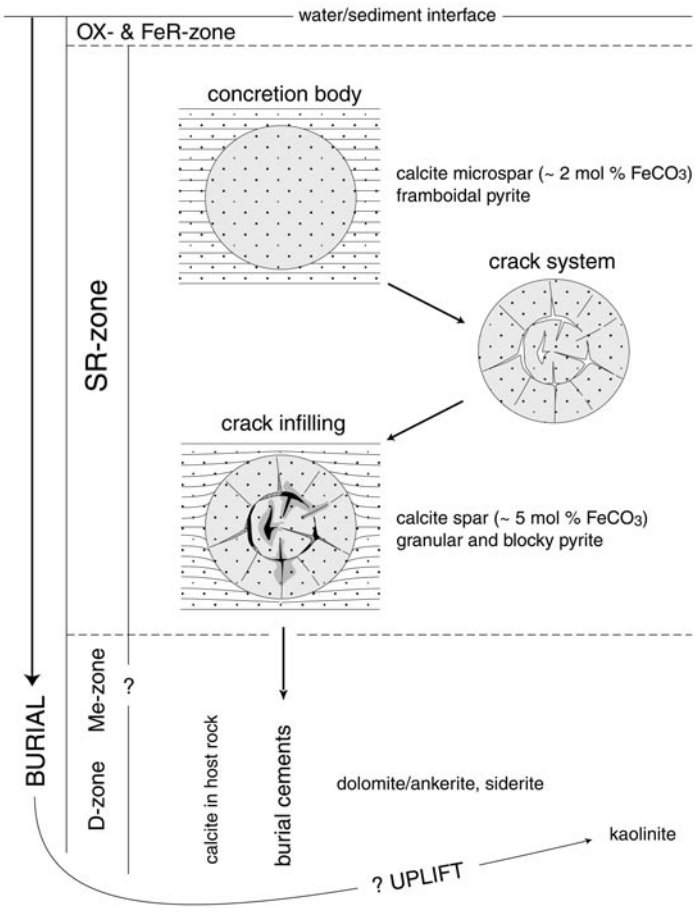

Fig. 15. Scheme showing stages of diagenetic formation of "cannon-ball" concretions in the Carolinefjellet Formation. *OX-*, *FeR-*, *SR-*, *Me-*, and *D-zones* are oxic, iron reduction (suboxic), sulphate reduction, methanogenic, and decarboxylation zones, respectively. For other explanations see the text.

Kaolinite is the last cement revealed in "cannon-ball" concretions, where it forms vermicular aggregates in rudimentary pores in cracks. Similar kaolinite infillings of rudimentary pores are known from other parts of the Adventdalen Group (Krajewski 2000a, b, Krajewski *et al*. 2001). This suggests their common origin in the Mesozoic sequence. It is likely that kaolinite precipitated as a result of diagenetic processes that operated during post-Early Cretaceous uplift of Spitsbergen.

Conclusions

The Kapp Morton section in Van Mijenfjorden gives insight into development of the "cannon-ball" concretions in the Carolinefjellet Formation in Spitsbergen.

The results of a combined sedimentologic, petrographic and geochemical study presented in this paper aid in elucidating their origin. They can be summarized by listing the most important events related to the formation and diagenetic history of the concretions. These events can confidently be placed in a relative time sequence embracing early to late diagenesis of the Carolinefjellet Formation (Fig. 15).

(1) The concretion bodies commenced to form in subsurface environment in OC-rich, fine-grained sediment column as a result of punctuated cementation of uncompacted sediment by non-ferroan (up to 2 mol% $FeCO_3$) calcite microspar. This cementation occurred in the upper part of the SR-zone, where high rates of hydrogen sulphide production led to formation of framboidal pyrite. Bacterial oxidation of organic matter as a result of sulphate reduction provided most of carbon dioxide necessary for concretionary calcite precipitation ($\delta^{13}C_{CaCO3} \approx -21‰$ VPDB). Perfect ball-like shapes of the "cannon balls" originated at this stage, reflecting pervasive cementation in permeable sediment at local sites of enhanced decomposition of organic matter.

(2) (Semi)indurated concretion bodies cracked under continuous burial as a result of amplification of stress around concretions in a more plastic sediment. The crack systems were combinations of septarian and spherical cracks, and they provided space for further precipitation of diagenetic minerals. The cracks were formed early in the sediment column, still in the SR-zone.

(3) Continuing calcite cementation of the concretion bodies was associated with precipitation of non-ferroan (up to 5 mol% $FeCO_3$) calcite spar and blocky pyrite in the crack systems. These minerals formed in deeper parts of the SR-zone under decreasing rates of bacterial sulphate reduction associated with progressive closure of diagenetic environment. Bacterial oxidation of organic matter was still the major source of carbon dioxide for calcite precipitation ($\delta^{13}C_{CaCO3} \approx -19‰$ VPDB). Precipitation of blocky pyrite was associated with local dissolution of calcitic matrix and formation of pyritization zones composed of microgranular pyrite. Compaction of hosting sediment led to mechanical deformations at margins of the concretions, and terminated their growth. At this stage, the "cannon-ball" concretions attained their final shape and texture.

(4) Subsequent stages of concretion evolution involved burial cementation of rudimentary pore space with diagenetic carbonates (dolomite/ankerite, siderite, calcite) under increased temperature ($\delta^{18}O_{Ca,Mg,FeCO3} \approx -14‰$ VPDB). Carbon dioxide for mineral precipitation was derived from thermal degradation of organic matter and from dissolution of skeletal carbonates ($\delta^{13}C_{Ca,Mg,FeCO3} \approx -8‰$ VPDB).

(5) Kaolinite cement precipitated as the last diagenetic mineral in the "cannon-ball" concretions, most probably during post-Early Cretaceous uplift of the sequence.

Acknowledgements. — The field work in Van Mijenfjorden (summer 2002) was supported by a research project No. 6PO4D04120 of the State Committee for Scientific Research. We thank Bożena Łącka, Michał Kuźniarski, and Ryszard Orłowski for isotopic, X-ray, and spec-

troscopic analyses, respectively. The carbon and oxygen isotopic analysis was done at the Stable Isotope Laboratory of the Polish Academy of Sciences in Warszawa. The paper benefited from reviews by Krzysztof Birkenmajer and Paweł Leśniak.

References

ASTIN T. R. 1986. Septarian crack formation in carbonate concretions from shales and mudstones. Clay Minerals 21: 617–631.

ASTIN T. R. and SCOTCHMAN I. C. 1988. The diagenetic history of some septarian concretions from the Kimmeridge Clay, England. Sedimentology 35: 349–368.

BECKER R. H. and CLAYTON R. N. 1976. Oxygen isotope study of a Precambrian banded iron-formation, Hamersley Range, Western Australia. Geochimica et Cosmochimica Acta 40: 1153–1165.

BERNER R. A. 1985. Sulphate reduction, organic matter decomposition and pyrite formation. Philosophical Transactions of Royal Society of London A315: 25–38.

CAROTHERS W. W., ADAMI L. H. and ROSENBAUER R. J. 1988. Experimental oxygen isotopic fractionation between siderite-water and phosphoric acid liberated CO_2-siderite. Geochimica et Cosmochimica Acta 52: 2445–2450.

COLEMAN M. L. and RAISWELL R. 1981. Carbon, oxygen and sulphur isotope variations in concretions from the Upper Lias of N.E. England. Geochimica et Cosmochimica Acta 45: 329–340.

COLEMAN M. L. and RAISWELL R. 1993. Microbial mineralization of organic matter: mechanisms of self-organization and inferred rates of precipitation of diagenetic minerals. Philosophical Transactions of Royal Society of London A344: 69–87.

COLEMAN M. L. and RAISWELL R. 1995. Source of carbonate and origin of zonation in pyritiferous carbonate concretions: evolution of a dynamic model. American Journal of Science 295: 282–308.

FRIEDMAN I. and O'NEIL J. R. 1977. Compilation of stable isotope fractionation factors of geochemical interest (Data of Geochemistry, Sixth Edition, Chapter K.K.). U.S. Geological Survey Professional Paper 440-KK, 12p.

HARLAND W. B. 1997. The Geology of Svalbard. Geological Society Memoir, London 17, 521 pp.

HESSELBO S. P. and PALMER T. J. 1992. Reworked early diagenetic concretions and the bioerosional origin of a regional disconformity within British Jurassic marine mudstones. Sedimentology 39: 1045–1065.

HJELLE A., LAURTITZEN Q., SVALVIGSEN O. and WINSNES T. S. 1986. Geological Map of Svalbard 1:100,000. Sheet B10G Van Mijenfjorden. Norsk Polarinstitutt, Oslo.

HOUNSLOW M. W. 1997. Significance of localized pore pressures to the genesis of septarian concretions. Sedimentology 44: 1133–1147.

IRWIN H., CURTIS C. and COLEMAN M. 1977. Isotopic evidence for source of diagenetic carbonates formed during burial of organic-rich sediments. Nature 269: 209–213.

KRAJEWSKI K. P. 2000a. Early diagenetic collapse and injection microstructures in phosphate nodules of the Brentskardhaugen Bed (Jurassic) in Spitsbergen. Bulletin of the Polish Academy of Sciences, Earth Sciences 48: 209–229.

KRAJEWSKI K. P. 2000b. Diagenetic recrystallization of apatite in phosphate nodules of the Brentskardhaugen Bed (Jurassic) in Spitsbergen. Bulletin of the Polish Academy of Sciences, Earth Sciences 49: 71–87.

KRAJEWSKI K. P. 2002. Catagenic ankerite replacing biogenic calcite in the Marhøgda Bed (Jurassic), Sassenfjorden, Spitsbergen. Polish Polar Research 23: 85–99.

KRAJEWSKI K. P. (*submitted*). Carbon and oxygen isotopic survey of diagenetic carbonate deposits in the Agardhfjellet Formation (Jurassic) in Spitsbergen: preliminary results. Polish Polar Research.

KRAJEWSKI K. P., ŁĄCKA B, KUŹNIARSKI M., ORŁOWSKI R. and PREJBISZ A. 2001. Diagenetic origin of carbonate in the Marhøgda Bed (Jurassic) in Spitsbergen, Svalbard. Polish Polar Research 22: 89–128.

MØRK A., DALLMANN W. K., DYPVIK H., JOHANNESSEN E. P., LARSSEN G. B., NAGY J., NØTTVEDT A., OLAUSSEN S., PČELINA T. M. and WORSLEY D. 1999. Mesozoic lithostratigraphy. *In*: W. K. Dallmann (ed.), Lithostratigraphic Lexicon of Svalbard. Review and Recommendations for Nomenclature Use. Upper Palaeozoic to Quaternary Bedrock. Norsk Polarinstitutt, Tromsø, p. 127–214.

MOZLEY P. S. and BURNS S. J. 1993. Oxygen and carbon isotopic composition of marine carbonate concretions: an overview. Journal of Sedimentary Petrology 63: 73–83.

NAGY J. 1970. Ammonite faunas and stratigraphy of Lower Cretaceous (Albian) rocks in southern Spitsbergen. Norsk Polarinstitutt Skrifter 152: 1–58.

PARKER J. R. 1967. The Jurassic and Cretaceous sequence in Spitsbergen. Geological Magazine 104: 487–505.

PRATT B. R. 2001. Septarian concretions: internal cracking caused by syn-sedimentary earthquakes. Sedimentology 48: 189–213.

RAISWELL R. 1982. Pyrite texture, isotopic composition and the availability of iron. American Journal of Science 282: 1244–1263.

RAISWELL R. and FISHER Q. J. 2000. Mudrock-hosted carbonate concretions: a review of growth mechanisms and their influence on chemical and isotopic composition. Journal of the Geological Society, London 157: 239–251.

ROSENBAUM J. and SHEPPARD S. M. 1986. An isotopic study of siderites, dolomites and ankerites at high temperatures. Geochimica et Cosmochimica Acta 50: 1147–1150.

SASS E., BEIN A. and ALMOGI-LABIN A. 1991. Oxygen-isotope composition of diagenetic calcite in organic-rich rocks: evidence for ^{18}O depletion in marine anaerobic pore water. Geology 19: 839–842.

SCOTCHMAN I. C. 1989. Diagenesis of the Kimmeridge Clay Formation, onshore UK. Journal of the Geological Society, London 146: 285–303.

SCOTCHMAN I. C. 1991. The geochemistry of concretions from the Kimmeridge Clay Formation of southern and eastern England. Sedimentology 38: 79–106.

SELLÉS-MARTÍNEZ J. 1996. Concretion morphology, classification and genesis. Earth-Science Reviews 41: 177–210.

Received 8 October 2003
Accepted 3 November 2003